GEOMORPHOLOGY AND RELATIVE AGES OF CHANNEL BELT DEPOSITS IN JEZERO'S WESTERN DELTA.

R. E. Kronyak,[1] K. M. Stack,[1] S. F. Sholes,[1] V. Z. Sun,[1] S. Gupta,[2] D. L. Shuster,[3] G. Caravaca[4] [1]Jet Propulsion Laboratory, California Institute of Technology, 4800 Oak Grove Drive, Pasadena, CA 91109 (rachel.e.kronyak@jpl.nasa.gov), [2]Imperial College, London, UK, [3]UC Berkeley, Berkeley, CA, [4]IRAP, Toulouse, France

Introduction: The western delta [1] in Jezero crater is composed of a sequence which includes finely layered planar strata, truncated curvilinear strata, and blocky deposits [2], interpreted as prodelta deposits, laterally accreting point-bars formed in meandering channels, and coarse-grained fluvial channel belt deposits, respectively [3-5]. The Mars 2020 *Perseverance* rover is completing its investigation of the lowest strata exposed within the western delta scarp [6], and will soon embark on a traverse across the delta "top," during which it will encounter these curvilinear strata and "blocky" channel belt deposits.

Here we use orbiter images and digital terrain models to map and characterize the ridge-forming blocky deposits of the western delta, reconstructing the time-order of channel belt deposition within the upper delta. We also re-examine the stratigraphic relationship between the ridges and the underlying curvilinear and planar layered deposits, as well as the largest impact craters on the top surface of the delta.

Data and Methods: Ridges were mapped at a scale of 1:5,000 using a 25 cm/pixel HiRISE basemap and a 1 m/pixel HiRISE digital terrain model [7,8]. Ridges were identified as linear to curvilinear features standing in high relief compared to the surrounding terrain. These deposits were mapped across the delta and grouped into distinct channel belt deposits based on common directions or inferred shared nodes.

A mineralogical analysis was performed with data from the Compact Reconnaissance Imaging Spectrometer for Mars (CRISM) by first converting spectral cube radiance to reflectance values. Corrections for directional lighting and atmospheric effects were then applied. The mean spectrum of each channel belt was collected and compared with mean spectra from other deposits.

Results: *Channel belt mapping:* Ridges comprise most of the western delta's top surface and also occupy the distal region of the Neretva Vallis inlet channel. Erosion has removed considerable portions of these deposits, particularly in areas to the southeast of Belva crater, where underlying truncated curvilinear strata are exposed.

Across the delta and within Neretva Vallis, 24 individual deposits were identified on the basis of similarities in morphology, texture, and inferred flow direction (Fig. 1). The majority of channel deposits occupy the main body of the delta to the south of Neretva Vallis and trend towards the southeast. Several exposures, however, are present within the Neretva Vallis channel (e.g., 'c' and 'f'), whereas others (e.g., 'd,' 'e,' 'x') extend to the northeast. Deposits 'a' and 'b' are distinct from the primary delta structure and are observed to the north of Neretva Vallis.

The best-preserved deposits (e.g., 'h,' 'k,' 'q') originate from distinct apexes proximal to Neretva Vallis and exhibit a fan-shaped morphology. Other

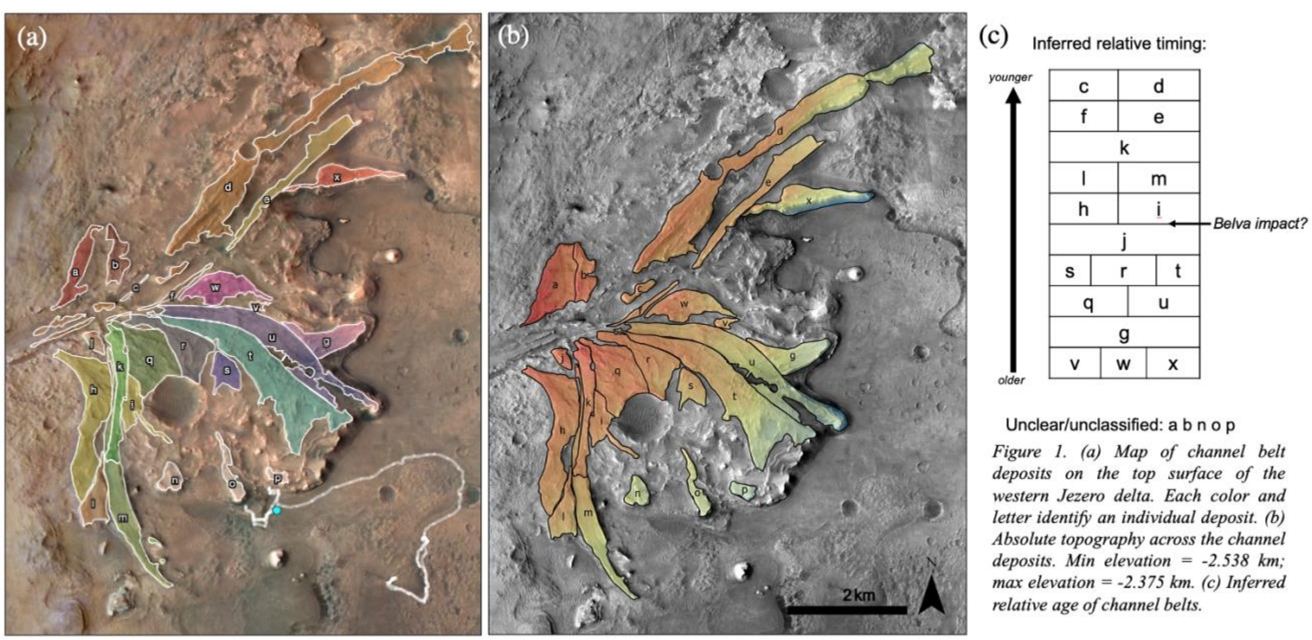

Figure 1. (a) Map of channel belt deposits on the top surface of the western Jezero delta. Each color and letter identify an individual deposit. (b) Absolute topography across the channel deposits. Min elevation = -2.538 km; max elevation = -2.375 km. (c) Inferred relative age of channel belts.

deposits are extensively eroded, leaving only remnants of ridge forms. In particular, boundaries between deposits in the central delta region (e.g., 'q-u') are challenging to define. In most cases, deposits observed on either side of topographic breaks were given unique deposit designations (e.g., 'r' and 's;' 'w' and 'v'), with the exception of the group of ridge and mesa deposits that occupy Neretva Vallis (i.e. 'c'). Relative ages were assigned based on cross-cutting relationships and inferred truncation surfaces between individual deposits. Some of the inferred oldest deposits (e.g., 'g' and 'x') exhibit distinct flow directions relative to overlying deposits.

Stratigraphic relationships in and around Belva crater: Belva crater, the prominent ~900 m crater on the southern surface of the western Jezero deposit, along with several other large nearby craters fall along an ~3.5 Ga isochron [9]. We observe blocky deposits from deposits 'q' and 'r' in the northern wall of Belva crater, but only curvilinear deposits in the southern rim of the crater (Fig. 2). Deposit 'i' west of Belva appears to abut sharply the curvilinear deposits that from the southern crater rim, and is not observed within the crater wall, instead appearing to curve around the southwestern portion of the Belva rim.

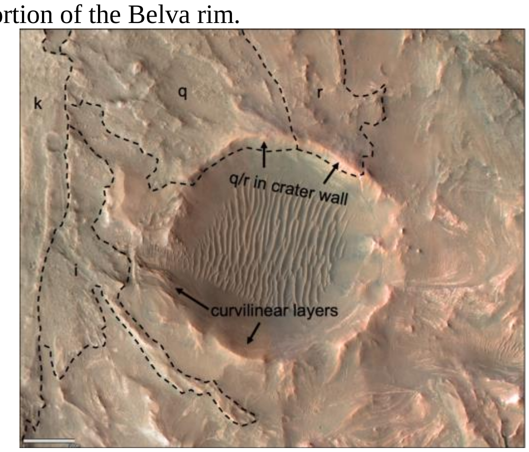

Figure 2. Channel belt deposits (dashed lines) annotated in and around Belva crater. Note that deposit 'i' skirts the southwestern rim of the crater and does not appear to be exposed within it.

Channel belt mineralogy: Mean CRISM spectra were extracted for each channel belt deposit. Consistent with previous studies, the deposits show absorptions corresponding to olivine/pyroxene and hydrated minerals like Fe- and Mg-bearing phyllosilicates and Fe/Mg carbonates [10,11]. Some deposits exhibit slight band depth variations that may correspond to lesser or greater proportions of Mg carbonate relative to Fe/Mg phyllosilicates (i.e., the 2.47 micron absorption strength relative to the 2.3 micron absorption). Deposits 'd,' 'e,' 'g,' 't,' and 'x' may be relatively more carbonate-bearing, while deposits 'a,' 'h,' and 'j' may be dominated by phyllosilicates. Other spectral variations between deposits may indicate differences in particle size. Further quantitative work will help to confirm and quantify these initial observations.

Discussion and Implications for Mars 2020 Exploration: The depositional sequence reconstructed here locates the oldest channel belt deposits ('v,' 'w,' and 'x') in the northern part of the western delta. A progressive sequence of deposits in the southern part of the western deposit beginning with 'g' and ending with 'k' followed. Based on relative relationships within and near Belva crater, we propose that Belva may have formed after the deposition of 'q' and 'r,' but before deposit 'i.' If this the case, Belva provides a critical chronometer for the deposition of the channel belt deposits, and may suggest a significant hiatus within this depositional sequence. The youngest deposits to form are those within Neretva Vallis and its northeastern extension.

The recognition of a time-ordered sequence of deposits within the delta is an important consideration for the Mars 2020 mission's exploration in Jezero. Although the sedimentary facies present in these channel belt deposits may be similar across the delta, each individual deposit has the potential to record a distinct depositional interval during the evolution of the Jezero delta, and individual deposits may record systematic variations in provenance over time.

Perseverance is expected to ascend the delta near deposits 'o' and 'p,' and traverse generally to the northwest, eventually making it to the Jezero crater marginal unit. Although it is not clear how 'o' and 'p' relate to the rest of the channel belts, these may represent relatively older deposits based on their low elevation and the potential for compensational stacking within the system. Perseverance is likely to encounter several of the relatively young channel deposits (e.g., 'h,' 'i'), with deposit 'k' representing the youngest to be investigated.

Acknowledgments: We acknowledge the early contributions of Axel Noblet, who drafted the first map of the western delta channel deposits during his 2019 JPL internship with K. Stack [12].

References: [1] Fassett, C. I. and Head, J. W., (2005), *GRL*. [2] Stack, K. M. et al. (2020) *Space Sci. Rev*. [3] Schon et al. (2012), *PSS, 67*, 28-45, [4] Goudge, T.A. et al. (2017), *EPSL, 458*, 357-365, [5] Goudge, T.A., et al, (2018), *Icarus 301*, 58–75. [6] Williams, A. et al., this meeting. [7] Calef et al. HiRISE basemap, [8] Calef et al. HiRISE DTM, [9] Mangold et al., 2020, Astrobiology. [10] Ehlmann, B. et al. [2008] *Nature, 1*, 355-358, [11] Horgan, B. et al. (2019), *Icarus, 339*, 113526. [12] Noblet, A. et al. (2020), DOI 10.5281/zenodo.3762958